

Multi-ttach: Techniques to Enhance Multi-material Attachments in Low-cost FDM 3D Printing

Nahyun Kwon*
nahyunkwon@tamu.edu
Texas A&M University
College Station, USA

Himani Deshpande*
hdeshpande11@tamu.edu
Texas A&M University
College Station, USA

Md Kamrul Hasan
kamrul05@tamu.edu
Texas A&M University
College Station, USA

Aryabhat Darnal
adarnal@tamu.edu
Texas A&M University
College Station, USA

Jeeun Kim
jeeun.kim@tamu.edu
Texas A&M University
College Station, USA

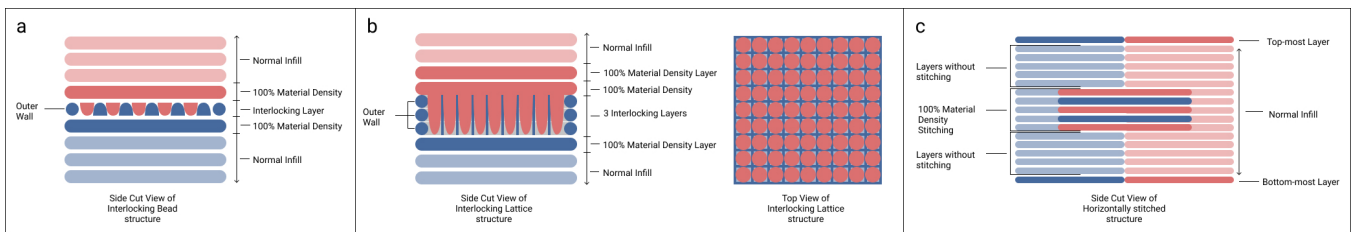


Figure 1: Multi-ttach is a novel printing technique to improve adhesion between mechanically dissimilar materials in 3D printed objects. We propose two vertical adhesion techniques of (a) Bead and (b) Lattice structure, and (c) Horizontal stitching.

ABSTRACT

Recent advances in low-cost FDM 3D printing and a range of commercially available materials have enabled integrating different properties into a single object such as flexibility and conductivity, assisting fabrication of a wide variety of interactive devices through multi-material printing. Mechanically different materials such as rigid and flexible filament, however, display issues when adhering to each other making the object vulnerable to coming apart. In this work, we propose Multi-ttach, a low-cost technique to increase the adhesion between different materials utilizing various 3D printing parameters with three specialized geometric structures: (1) bead and (2) lattice structures that interlock layers in vertical material arrangement, and (3) stitching in horizontal material arrangement. We approach this by modifying the geometry of the interface layer at the G-code level and using processing parameters. We validate the result through mechanical testing using off-the-shelf materials and desktop printers and demonstrate the applicability through a range of existing applications that tackle the benefit of multi-material FDM 3D printing.

*Both authors contributed equally to this research.

Permission to make digital or hard copies of all or part of this work for personal or classroom use is granted without fee provided that copies are not made or distributed for profit or commercial advantage and that copies bear this notice and the full citation on the first page. Copyrights for components of this work owned by others than ACM must be honored. Abstracting with credit is permitted. To copy otherwise, or republish, to post on servers or to redistribute to lists, requires prior specific permission and/or a fee. Request permissions from permissions@acm.org.
SCF '21, October 28–29, 2021, Virtual Event, USA

© 2021 Association for Computing Machinery.
ACM ISBN 978-1-4503-9090-3/21/10...\$15.00
<https://doi.org/10.1145/3485114.3485116>

CCS CONCEPTS

• Human-centered computing → Interactive systems and tools.

KEYWORDS

3D printing, multi-material, adhesion, fabrication

ACM Reference Format:

Nahyun Kwon, Himani Deshpande, Md Kamrul Hasan, Aryabhat Darnal, and Jeeun Kim. 2021. Multi-ttach: Techniques to Enhance Multi-material Attachments in Low-cost FDM 3D Printing. In *Symposium on Computational Fabrication (SCF '21), October 28–29, 2021, Virtual Event, USA*. ACM, New York, NY, USA, 13 pages. <https://doi.org/10.1145/3485114.3485116>

1 INTRODUCTION

To date, advances in low-cost 3D printer machinery and the progress in materials manufactured for Fused Deposition Modeling (FDM) printing have made it possible to expand the range of 3D printable artifacts by non-experts. Integrating various material-specific characteristics and leveraging both single (e.g., Prusa [Průša 2021], Ender 3 [Creality 2018]) and dual extruder FDM printers (e.g., Flashforge [Flashforge 2016], Ultimaker [Ultimaker 2016]), recent work has tackled techniques to create practical applications using multi-material printing, for example, shape changing applications [An et al. 2018; Tahouni et al. 2020], assistive attachment devices [jtronics (Thingiverse user) 2019; Kim et al. 2017] and mechanical devices [Yusuf 2017]. While multi-material printing could be more versatile in advanced 3D printers similar to Polyjet (e.g., Stratasys Objet Series [Scala 2020]) and single extruder with multiple feeders (e.g., Builder Extreme Series [Builder 2019]), and even though the accessibility of those machines is gradually improving, most end

users are yet equipped with low-cost, single extruder machines. Furthermore, many still experience practical issues to get successful multi-material printing with the dual extruder, such as oozing, misalignment of models, or clogging of extruders (e.g., [parakartracer (Zortrax Forum user) 2020] [tnorton (Simplify3D Forum user) 2019], [tSaK (Raise3D Community user) 2018]). One of the major issues within the low-cost FDM 3D printing is the adhesion between two layers of mechanically dissimilar materials such as rigid plastic attached to a flexible material. Objects having these different materials with low adhesion property cannot withstand stresses and thus easily come apart in practice.

We propose Multi-ttch, a novel computational approach to revise pre-sliced structures of G-code to print multiple materials, which can be applied at the contact layers of two dissimilar materials to enhance the inter-material adhesion. Our method is not only valid for dual extruder printers which are becoming more accessible along with the decreasing cost, but also valid for single extruder printers. We address what we term as ‘vertical adhesion issues’ between layers that occur when a material layer is printed on top of another material layer, and ‘horizontal adhesion issues’ between two dissimilar materials printed next to each other where a single layer of the print may have multiple materials (see Figure 1). We take pre-sliced files of multi-material print using commercial slicing programs (e.g., Cura [Braam and Ultimaker 2017], Slic3r [Ranellucci 2018]) with verbose comments as input and modify the code at the contact area, replacing it with interlocking structures that help to hold the two materials tight. We provide two structures to enhance the vertical adhesion, namely, interlocking bead and lattice structures, and a stitching structure to enhance horizontal adhesion. We validate the result through tensile testing, and showcase various application examples. We also offer users an interactive editor, where they can upload pre-sliced G-code using commercial slicing programs then obtain a ready-to-print Gcode file with modified printing paths to enhance bonding. We conclude with discussion about the limitations and proposal of future work.

2 BACKGROUND & RELATED WORK

2.1 Increasing Needs in Multi-material Printing

Multi-material printing refers to using different material filaments in a single print job, where a filament is swapped according to the material selected for the parts of a 3D model design. The availability of advanced materials [Simplify3D 2019] in low-cost FDM 3D printing has not only expanded the capability of this accessible technology, but also showcased the potential of combining these materials through a 3D printed object to impart it with interesting abilities. Researchers have discovered the promise of multi-material printing through mechanically reversible and foldable objects [Noma et al. 2020], combining flexible and hard structures for printing anatomical models [Smith and Jones 2018], and shape-changing composites [An et al. 2018; Tahouni et al. 2020]. Further with the advent of low cost FDM printer machinery, multi-material printing has permeated into makers’ design space by enabling them to print objects in different colors for aesthetic purpose [nervoussystem (Thingiverse user) 2014; r3ND3R (Thingiverse user) 2015; ramooown (Thingiverse user) 2015], and rigid and flexible properties together

[Punished-Props-Academy 2017]. It is also used for printing dissolvable supports, that can mimic high-end printers that were only available for experts and practitioners [Dwamena 2021].

To fast forward to the hardware approach, modifying or updating the extruder has enabled researchers to create robust custom electronic circuitry [Butt et al. 2018], high-end 3D printers for industrial use with multi-extruders has enabled printing of complex interactive artifacts such as multi-material robots [Skylar-Scott et al. 2019], and facilitated FDM dual-material printing with improved bond strength using an intermixer to mix the different material filaments [Khondoker et al. 2018]. Commercial add-ons for desktop printers such as Mosaic Palette [Mosaic-Manufacturing 2021] offer a way to use multiple materials on a single nozzle FDM printer. Yet, these methods either require expensive machine or hardware updates that are not viable for all end users with desktop printers.

To accommodate the increasing thirst to 3D print artifacts in multiple materials, recent work has tackled various approaches for end users to serve multi-material printing as a single job. Different open-source slicing software have the functionality to prepare STL files for multi-material printing. Replicator G [Smith et al. 2011] offers combining the G-code of two separate STL files to create the dual-material G-code. MeshMixer [Mosaic-Manufacturing 2017] allows users to split a single STL file that is not originally prepared for multi material printing into parts. Programmable Filament [Takahashi et al. 2020] makes multi-material printing possible and accessible for low cost, single extruder FDM 3D printers, through simply a software approach of modifying the G-code.

All in all, this body of work has gone into enabling multi-material 3D printing owing to its rising potential in reducing the otherwise high manufacturing cost to produce different applications, making it more and more essential. As desktop FDM multi-material printing becomes increasingly accessible and widespread, addressing the technical challenges with respect to the adhesion issues between dissimilar materials would help makers in printing stronger and durable multi-material artifacts.

2.2 Tackling Adhesion Issues in Mechanically Distinct Materials for FDM Printing

Since low-cost FDM 3D printing has opened the doors for manufacturers and scientists to experiment with the advanced materials that can be created as filaments, to date, materials of different chemical and mechanical abilities have become commercially available for anyone to purchase. Apart from the commonly used Polylactic Acid (PLA) and Acrylonitrile Butadiene Styrene (ABS), materials with flexibility such as Thermoplastic Polyurethane (TPU) and Nylon, water-solubility such as PolyVinyl Alcohol (PVA), and different textures such as wood and metal are available on the market [Simplify3D 2019]. Materials with advanced capabilities such as conductivity [Flynt 2018a], magnetic properties [Flynt 2018b], as well as shape-memory properties [Kyoraku Co. 2017], have become available for commercial use.

However, due to the discontinuous nature of FDM that deposits molten polymer layer by layer, assuring mechanical properties has been a challenge in FDM [Garg et al. 2014]. When the printer extrudes the molten fiber, the previous layer is solidified with rapid cooling, which causes the interface to not be fused enough with

the next layer. Eventually it leaves voids between filaments and the interface loses mechanical properties that ensure a stable bonding [Ahn et al. 2002; Coogan and Kazmer 2017; Thomas and Rodríguez 2000]. Although there have been many endeavors to increase mechanical strength of FDM parts (i.e., development of novel materials [Dul et al. 2018; Roberson et al. 2015], parameter optimization [Ravi et al. 2016]), the weakly adhered interface of two different materials in a single model still remains critical due to different properties. From this body of work, we can see that there may exist various reasons causing adhesion issues at junctions. The ‘merged meshes overlap’ feature of Cura [Braam and Ultimaker 2017] may be a respite from weak adhesion but the feature essentially ‘squishes’ the input 3D files together requiring a user to consider the size of input models or redesign them (e.g., two hemispheres with offset parts in the center to form a perfect sphere). Apart from putting the onus on the user to design with added tolerances, this feature affects the shape, size and the outer aesthetic of the final object. Furthermore, it does not work for vertically stacked objects.

We address the adhesion issues by taking two major approaches of touching upon printing parameters and a geometric approach to retain the shape, size and outer aesthetic of the final object, following the knowledge obtained from previous work as is outlined in the next section.

3 UNDERSTANDING FACTORS THAT AFFECT ADHESION BETWEEN TWO MATERIALS

There have been several studies that have investigated printing parameters to increase bonding strength between mechanically different polymers. Among many, we count four factors that are studied in depth presenting a greater impact in the final artifacts.

Print Bed Temperature. Increasing the temperature of a printing bed has been recognized to remarkably increase the bonding strength of the interface by 93% [Yin et al. 2018]. The study also shows that increasing a nozzle temperature and a printing speed can strengthen the bonding strength, but their impact is relatively negligible compared to modification of the bed temperature. Lowering layer thickness is also helpful by reducing the gradients of temperature change in layers laid down between the bed and the nozzle. It manifests that retaining high temperature of the 3D printed solids on the bed helps the next layer to easily adhere to the previous one. They however used particularly thin sample to test the adhesion strength. As flat 3D objects can easily get affected by the heat from the printing bed, we can infer that we may need another technique to mimic the impact for real-world examples with a larger Z-height.

Material Density and Interlocking Geometry. Another recommendation was printing the second material into the infill section of the last three layers of the first material with 100% material density. This creates an interlocking structure between the two materials before proceeding to print the first three layers of the second material with 100% material density infill [Tamburrino et al. 2019]. For dual material printing with a single nozzle printer, we can interpret this as having 3 interlocking layers with 100% material density followed by 3 layers of the second material with 100% material density.

voids/Discontinuity in Geometry. The roughness on the interface surfaces constitutes to the adhesion theory of mechanical interlocking. Depending on the material property, if the material

is brittle, the surface roughness reduces the practical adhesion whereas if the material is ductile, the roughness improves practical adhesion due to local plastic deformations [Da Silva et al. 2011; Mittal and Pizzi 1999]. Since we are looking at FDM polymer filaments which are ductile by nature, it would follow that adding interlocking structures would improve the adhesion.

Printing Order. While it was suggested to further investigate about the reasoning, one recommendation is to print the rigid material first and the flexible material next [Tamburrino et al. 2019].

With these known-recommendations, we take a step further in designing techniques to print an artifact with multiple materials vertically and side-by-side. To assist users in creating stronger multi-material bonds, our processes use existing desktop FDM machines and modify the G-code of the sliced CAD models by a hybrid method of adding interlocking geometry at the interface layers and modifying printing parameters such as extrusion amount and printing path, bypassing any hardware considerations. We propose a contribution over existing work [Tamburrino et al. 2019] in terms of possible UX affordances by covering various shapes, structures, and alignments of the model. While [Tamburrino et al. 2019] covers only vertical adhesion in an ideal square shape, real-world 3D objects present multiple, irregular or organic shapes and varying alignment at the interface. Our proposed method handles those variations in vertical and horizontal adhesion scenarios. We also propose a web-based interactive editor to make these findings accessible to end users.

4 MULTI-TTACH: TECHNIQUES FOR MULTI-MATERIAL ADHESION

Multi-material printing using a single nozzle FDM printer is achieved often by pausing the print in the middle of layers where the user might want to change the material and switch out the filament (i.e., [Takahashi et al. 2020]). As investigated in the previous work, geometric approach that adds mechanically interlocking structure and non-geometric approaches (e.g., modification of infill density and slicing patterns [Tamburrino et al. 2019], increasing temperature of the print bed [Yin et al. 2018]) complement adhesion between two materials. We follow a hybrid approach of using the G-code to modify the geometry at the interface of two materials and printing parameters such as the print path and extrusion amount, to create interlocking structures with the two materials. By utilizing pre-sliced geometry as an input, our method can be inserted into existing slicers as a plug-in, or even operate as a post-processing software for any slicer, thus achieving versatility regardless of the type of slicer used. In the previous work [Takahashi et al. 2020], M0 command is used to pause the print and resume, where users need to manually switch out the filament for the next part of the print. Since some material from the previous filament might still be left in the extruder, material is purged before commencing the print job. The nozzle is then primed with the switched material, and the printing of the next layers can begin. As can be inferred from this, the manual switching process can inevitably take some time causing the last layers to cool down. It may result in lowered bonding strength between two layers. Following the existing approach and the empirical knowledge, we build Multi-ttach, a computational technique to improve the adhesion between different materials.

4.1 Heating Previous Layer

Poor adhesion issues are exacerbated with the higher temperature gap between two layers due to cooling while switching materials. Often the layer that is being printed adheres well to the previous layer through inter-layer wetting and diffusion [Bellehumeur et al. 2004; Sun et al. 2008; Turner et al. 2014] as they both are in glass state range before they are solidified [Wool and O'connor 1981]. As the time for material swap may cause decrease in temperature of previous layer, we heat the previous layer once again just after switching to the next filament, by repeating the extruder path of the previous layer without any extrusion but with a slightly lower Z-height. Heated extruder touches the top of the layer transmitting heat from the hot nozzle. Once the path is complete, the next layers immediately begin printing to minimize the time gap. Note that this process might not be necessary in dual extruder printers that maintain the printing temperature of both nozzles and leave no time gap to replace materials.

4.2 Adding Adhesion Structures by Modifying Interfacing Geometry

We adapt findings from [Tamburrino et al. 2019] to first interlock infill and outer wall. Following the idea, we propose three structures to modify the geometry of the interface layers, forming an interlocking geometry between two materials. Our algorithm only modifies the infill region while leaving the outer shell as it is, keeping the external appearance of the printed object as it is. To secure two vertically placed interface layers and have them tightly hold each other, we generate special geometry of 'bead' and 'lattice' structures, that we will detail in the following subsections. For horizontally placed regions of distinct materials in the same layer, we propose horizontal 'stitching', that can connect two regions using different materials alternatively.

4.2.1 Vertical Adhesion Structure 1: Bead. We start by creating a rough surface that consists of an array of beads with empty spaces at the adhesion layer. These empty spaces are then filled with another set of beads constructed by the second material, generated by purging the material while lifting the nozzle, as shown in Figure 2c. These offset beads from lower and upper layers lock with each other tightly. Due to geometric characteristics of these series of beads, we refer to these adhesion layers from the top and bottom in bead structure as 'lower crown layer' and 'upper crown layer'. Users may use different infill density and structures causing these beads to fall in through the hollow spaces in the infill and thus we cover these layers with a full infill layer (in 100% material density from top and bottom as illustrated in Figure 1a-b) before printing the crown layers with beads. The full infill layers also help flatten the top of beads and stick to the next normal layers. Figure 2 shows the step by step printing process of interlocking bead structure.

4.2.2 Vertical Adhesion Structure 2: Lattice. Similar to the bead structure, we start the lattice structure by creating empty spaces using the first material at the interfacing layer which are filled with the second material for interlocking. The main difference between bead structure and lattice structure is their lower interlocking layer; the lattice structure consists of a *bucket layer* instead of a *crown layer* as in the bead structure. We create a lattice pattern by generating

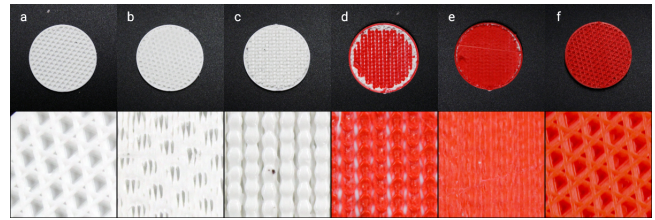


Figure 2: Step by step view of Bead structure printing process: (a) once normal infill layer is complete, (b) full infill layer covers (100% material density), (c) to print lower bead layer in material 1, then (d) offset to upper bead layer in material 2 and interlock each other. Finally (e) a full infill layer covers the bead layer to (f) print the rest in normal infill.

'buckets' with cross-sectional lines that replace the last three layers of the first material. Then the extruder travels through the center position over the top of the lattice and purges beads of the second material in each bucket forming the upper layer of the interlocking structure as shown in Figure 1b.

Similar to the bead structure, we add a full infill layer (in 100% material density) before lattice structure begins, ensuring any modified structure not to fall into the hollow regions in the previous layers with sparse infill. As beads purged into the lattice are discrete and thus might not get tightly attached to the next layer, we add another full infill at the same Z-height of where beads were made to increase bonding with each bead and also with the layer above. We cover bead layer with full infill layer to help it well-adhere to the next normal infill layer beyond our modified layers. Figure 3 illustrates the interlocking lattice structure.

4.2.3 Horizontal Adhesion Structure: Stitching. While the two geometric approaches above are useful for vertical material switching such as in bi-layer structures for many programmable shape changing specimens [jtronics (Thingiverse user) 2019], multi-material printing side by side or throughout several layers on a dual extruder printer can also be susceptible to poor adhesion. To address this, we also propose horizontal stitching, where we connect two infill regions at the interface of the two materials by overlapping lines across regions starting from each end in each material. Repeating throughout the layers that have multiple materials in them, we add a horizontal 'stitching' structure, as described in Figure 1c. This method is better suited for dual extruder printers. Although we do not add any additional material switching, such settings require the user to change the filament at every single layer if using the single extruder machine, which would not be ideal in practice. Figure 4 shows the example of horizontally stitched model in cut state.

4.3 Algorithm Implementation

We utilize Cura [Braam and Ultimaker 2017] as a slicing software to get an input G-code file. Cura generates verbose comments that indicate each part of the movement path such as '`;TYPE:WALL-INNER`' and '`;TYPE:FILL`' that we use as delimiters. Our method is applicable for other slicers (e.g., Slic3r, KISSlicer, Skeinforge) as long as they provide the corresponding comments. With a single STL file input that is not created for multi-material printing, our

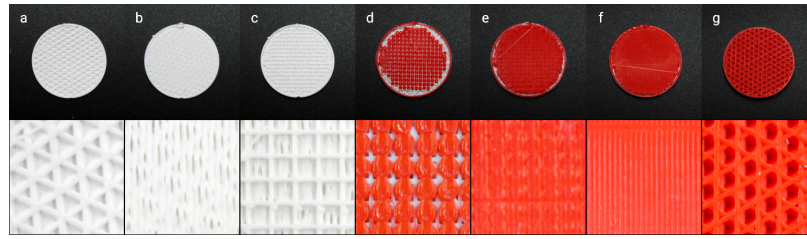


Figure 3: Step by step view of Lattice Structure: once complete with (a) normal infill layer, (b) full infill layer (100% material density) is covered to host (c) three layers forming bucket layers in first material, that will be (d-e) filled with second material by excessive purged material, then followed by lines to connect discrete beads in the same layer. (f) Another full infill layer with 100% material density covers the structure and then the (g) rest of the print continues in normal infill

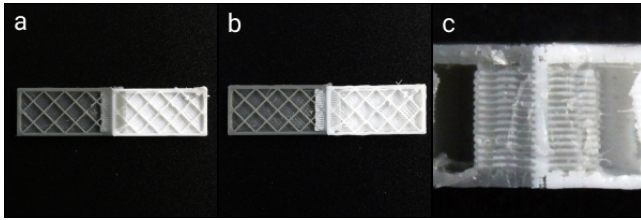


Figure 4: Step by step view of Horizontal Stitching structure: (a) stitching first material into second material (b) stitching second material into first material, (c) cross-section view of a horizontal stitch showing the two materials interlocking.

algorithm first finds the target layer (the layer at which the material will be switched) for adhesion structure that is specified by the user input (n) in the interactive editor by searching ‘;LAYER:[layer number = n]’. Yet, in the most common scenario, the user is likely to import multiple STL files split in parts or offset a single STL file into multiple parts using commercial software (e.g., MeshMixer [Mosaic-Manufacturing 2017]). If the user already owns the G-code file that is originally split in parts for multi-material printing, ‘Tn’ commands in the dual extruder settings are used in finding an exact location for material change. In this case, no user input is needed to specify a target layer. A user can choose between two options to add the adhesion structure based on the type of STL file they have. The user walkthrough will be detailed in Section 5.

4.3.1 Vertical Adhesion in Horizontal Plane: Bead and Lattice Structures. The two vertical adhesion structures—bead and lattice—have a similar vertically stackable architecture that consists of 4 components in brief: (1) full infill layer, (2) lower adhesion layer, (3) upper adhesion layer, and (4) full infill layer as abstracted in Figure 1. We assume that the G-code file was sliced with the absolute positioning mode (G90) and relative extrusion mode (M83) by default.

Searching Regions to Add Adhesion Technique. Generating two vertical adhesion structures starts from the same initial step of finding polygons that constitute the infill region at the target layer. The adhesion layer may present various shapes that may be more organic in nature. There could be multiple inner walls in a single layer with several closed loop polygons (e.g., Figure 5c), or nested empty polygons as an example shown in Figure 5d. Because the slicer generates G0 (moves the extruder while extruding the material) and G1 (moves the header without any extrusion) commands

only with any directional change of a vector along the extruder trajectory, we can simply connect all coordinates to find the inner wall’s shape outline in a closed loop.

Plotting Grid Coordinates in Various Shapes. Keeping only the coordinates at regular intervals in the valid inner wall region as illustrated with the blue dots in Figure 5, we set two constraints: (1) the points should be distant from all the points that construct inner wall polygons, at least by 1mm which guarantees that the adhesion structure avoids any disruption of the exterior appearance of the model; and (2) the points are discarded if they are located inside the empty inner polygons, addressing a 3D model with nested empty space. The second constraint avoids printing in holes that may be a part of the 3D model. For manipulation and analysis of planar geometric objects, we used Python package Shapely¹.

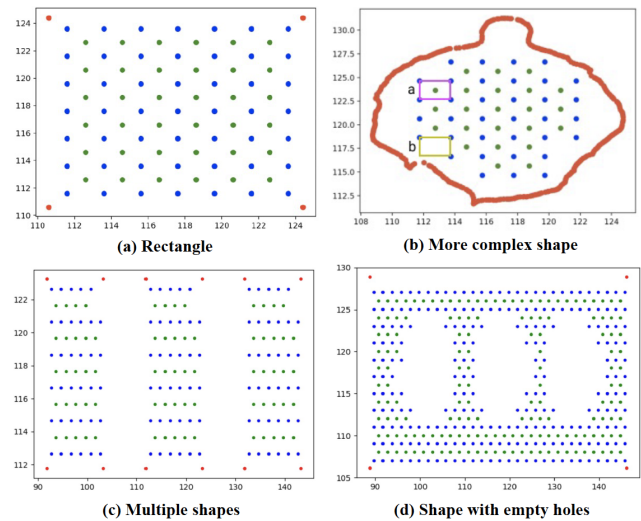


Figure 5: Visualization of the coordinates found from various polygon shapes with three colors: (1) red = edge coordinates of inner wall, (2) blue = lower grid coordinates, and (3) green = upper grid coordinates.

For two interlocking layers that hold each other from top and bottom, we need two different sets of offset coordinates for lower

¹<https://pypi.org/project/Shapely/>

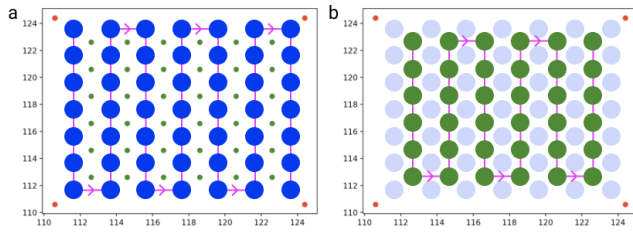


Figure 6: Generating the bead structure using grid coordinates: (a) lower crown layer – blue circles show extruded beads and pink lines show the tool path, (b) upper crown layer – green circles show extruded beads in the empty spaces and pink lines show the tool path

and upper adhesion layer. The grid coordinates that satisfy the two constraints constitute the lower adhesion layer for bead and lattice structure, that we term as ‘lower grid coordinates’. Then, we generate another set of grid coordinates (‘upper grid coordinates’) for the upper adhesion layer that are offset from lower grid coordinates to interlock printed structures. The algorithm iterates for the lower grid coordinates (blue dots in Figure 5) then generates the points for upper grid coordinates (green dots in Figure 5) to locate them at the center of each square found. Positioning of each dot in the empty space is confirmed only if there are 4 enclosing adjacent points that construct a square, such as 4 blue points that construct a pink square ‘a’ in Figure 5b. If there is any missing point among 4 points that form a square as in the yellow square ‘b’ in Figure 5b (one point is missing), the algorithm does not generate a coordinate at the center. This ensures enough space to put the next filament and prevents the space from being overflowed.

Generating Full Infill. The initial and final step to wrap adhesion structure is to add full infill layer below and above the adhesion layers. We employ the same algorithm of getting lower grid coordinates that is adjustable to any shape of polygons, but with the decreased gap between two coordinates (0.6mm). The extruder draws a line following these grid coordinates in y-axis in sequence (e.g., Figure 2b and Figure 2e). To save printing time and material cost, the algorithm generates thinner lines that moves faster than lines for printing bucket layers (see Figure 3b). We used equation 1 to compute the E value (the length of the filament that gets into the extruder) with the modified seed value 0.4, empirically found stable from experiments.

Generating Bead Structure. We first find the Z-height of the target layer by finding the Z-height from the section followed by the ‘;MESH:NONMESH’ comment of the target layer, and subtracting 0.2mm (assuming layer thickness is set to 0.2mm) from the value. The ‘;MESH:NONMESH’ section of a layer contains the Z-height of the next layer. Following the lower grid coordinates sequentially, we generate a set of G-code commands purging material at each coordinate in the lower layer while moving the header up by 0.4mm (equal to twice the layer height) from the current Z-height for every bead extrusion. After purging, the header returns back to the current layer’s Z-height subtracting 0.4mm from its value while moving to the next bead location. The E value of each bead has been set to

0.7mm empirically, not to over or under extrude material at each position. As illustrated in Figure 6a with pink lines, the printing path is in the zig-zag pattern by shifting its direction alternatively. This prevents the previous beads from being smashed by the extruder during its travel. The same mechanism goes for the upper crown layer, starting from the same Z-height as the lower crown layer.

Generating Lattice Structure. Bucket layers are generated by drawing lines following lower grid coordinates (Figure 7a-b). It also follows a zig-zag path not to affect empty spaces between printed lines with the drooping material from the extruder while moving to the next line. We use the following equation 1 to compute the E value for extrusion, with a seed value to adjust computation which we found stable at 0.08, empirically.

$$Extrusion = (LayerHeight * NozzleDiameter * Length * X) / FA \quad (1)$$

Where we use settings for layer height = 0.2mm, nozzle diameter = 0.4mm, length (travel distance) = 2mm, FA (area of longitudinal section of filament) = $(\text{filament diameter}/2)^2/\pi$, X (an empirical seed value to adjust extrusion amount) = 0.08.

Starting 3 layers below the target layer, the algorithm repeats to create lattice with a matrix of buckets with empty spaces. Upper crown layer locates one layer above the target layer, filling the buckets with the purged filaments in the next material. The extruder follows along upper grid coordinates and purges the constant amount of the material, which is set to 0.9mm. To ensure enough time to fill the buckets with the next material, the extruder travels in a slower feed rate (F50) while purging. As presented in Figure 7d, upper crown layer is followed by a full infill layer above the series of beads to connect them tightly, adding extra adhesion strength throughout the upper crown layer.

Finally, another full infill layer wraps the bead and lattice structure to help them stick to the next normal infill layer well.

Adding Pause Code for Material Exchange. For a single extruder printer, we added pause command (M0) which temporarily interrupts the printer operation letting users switch the material, and then resume the printing. M300 command makes a short beep sound notifying the user to switch the filament. If set by user through the interface, commands to change the printing temperature (M104 and M109) are also added, particularly when recommended printing temperatures of two materials are distinct. We employed the same mechanism with as Cura [Braam and Ultimaker 2017] of purging lines that prime the nozzle, but in a shorter and thicker line so that it does not knock off the printed model on the bed. The extruder moves up at the home location, to prevent it from hitting the model while returning to the original point diagonally.

4.3.2 Horizontal Adhesion Structure: Stitching. As introduced in Section 4.2.3, horizontal stitching can address adhesion issue of dissimilar materials placed side by side in the dual extruder printer setting. This ‘stitching’ algorithm generates a set of straight lines that connect two regions that are being printed in distinct materials horizontally (see Figure 4a-b), similar to a fabric stitching that mends two pieces of material with a thread.

Finding Regions that Interface Each Other. The stitching mechanism starts from finding all the layers that have multiple materials.

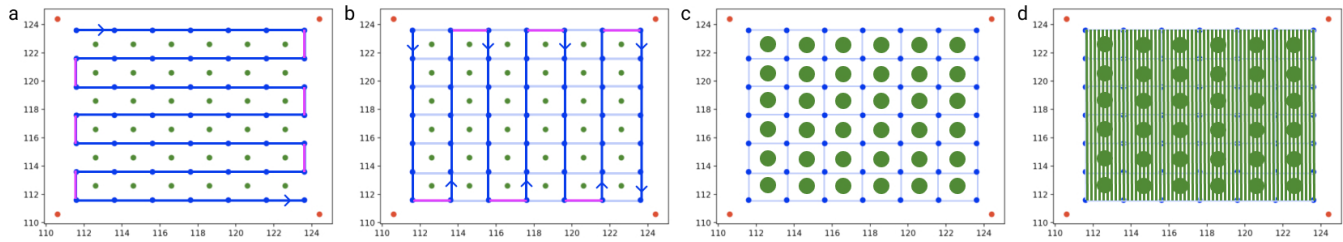


Figure 7: Generating the bucket layer for the lattice structure: following the blue grid coordinates in a zig-zag path to create buckets with the first material for the second material to be purged into (a-b) – blue lines indicate the extrusion path and the pink lines indicate movement of the nozzle without any extrusion. Generating the crown layer for the lattice structure: Following the green grid coordinates, the second material is purged into the buckets (c) followed by a 100% material density layer with the second material (d) – green circles and lines indicate extruded material

The layer with tool change command (Tn) for multiple extruders indicates that it has parts for multi-material printing. We skip the first and last 5 layers to ensure that the top covers are not stitched and retain the original exterior appearance. Our algorithm retrieves all commands to print outer walls of multi-material layers, which are critical to find the placements and planar relationships of each region. We first identify the adjoining parts of two multi-material regions that need stitching. The algorithm searches adjacent points of two closely located polygons. As these points for extruder trajectory are at the center-line of the printed line (line thickness tends to be the nozzle diameter—0.4mm—), this makes offset for two tightly attached lines in practice (e.g., points in red-colored region A in Figure 8a) to be less than 0.4mm. If the distance between two points (one from polygon of the first material and the other of the second material) is smaller than 0.4mm, those two points are considered to be right next to each other². We generate stitching mechanisms for these points only.

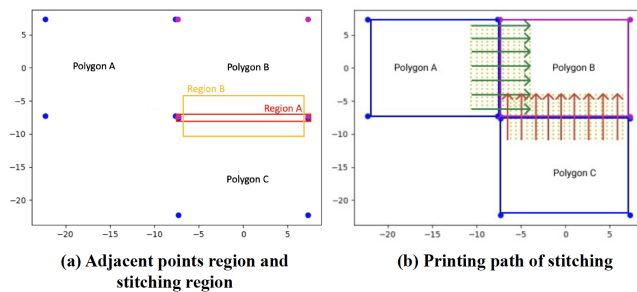


Figure 8: (a) Finding adjacent points (red dots) between two material regions. Region A is the smallest rectangle containing all adjacent points found in neighboring regions, region B is a rectangular area to stitch. (b) Generating horizontal stitching in three rectangles aligned vertically (B-C) and horizontally (A-B). The arrows show stitching directions.

Identifying Placements of Neighboring Regions. Identifying planar alignment of multi-material regions is significant to generate orthogonal lines that connect two regions as illustrated in Figure 8b.

²We assume the most common nozzle size as threshold but can be adjusted for thinner or thicker nozzle

We find the smallest region that contains all the adjacent points (e.g., region A in Figure 8a) to determine the planar relationship of two polygons (vertically or horizontally aligned in one plane).

Generating Stitching Lines. We identify a region to fill in with stitching lines, such as region B in Figure 8a, which intersects the region of adjacent points, region A. Extrusion amount and drawing lines follow the same algorithm of generating full infill, but orthogonal to the adhesion part to print lines that connect two distinct regions. As these horizontal lines are thin enough, we simply add stitching commands in multi-material layers without modifying any existing commands of the source G-code file or replacing existing infill.

5 INTERACTIVE EDITOR TO POST-PROCESS PRE-SLICED GCODE

For the end user accessibility, we provide a web-based interactive editor (Available at <https://multi-ttach.herokuapp.com/>), enabling users to upload their G-code file and add a desired adhesion structure (see Figure 9). Our interactive editor utilizes Python Flask³ as a backend framework. For overall frontend structure, we replicated the structure of gCodeViewer [hudson (Thingiverse user) 2012], which is an open source web application for G-code simulation in a 2D and 3D plane.

To initiate the use case, users would import a pre-sliced G-code file using Cura [Braam and Ultimaker 2017], either sliced for single material printing in a single extruder using one STL file, sliced for dual extruder setting using multiple STL files in parts even if they will eventually use the single extruder, or sliced for dual extruder with multiple STL files as input. ‘About’ tab shows instructions about the three available adhesion structures for users to choose.

Figure 10 illustrates a flow chart for the user workflow to generate an adhesion structure using the editor. There are three options available in the menu on the left side: (1) vertical adhesion structure in the single extruder setting, (2) vertical adhesion structure in the dual extruder setting, and (3) horizontal stitching in the dual extruder setting. Users can choose a desired option by clicking a dropdown box for each option. For (1) and (2), if users select vertical adhesion structure, they are granted further options to specify the type of adhesion structure: bead and lattice. The editor

³<https://flask.palletsprojects.com/en/1.1.x/>

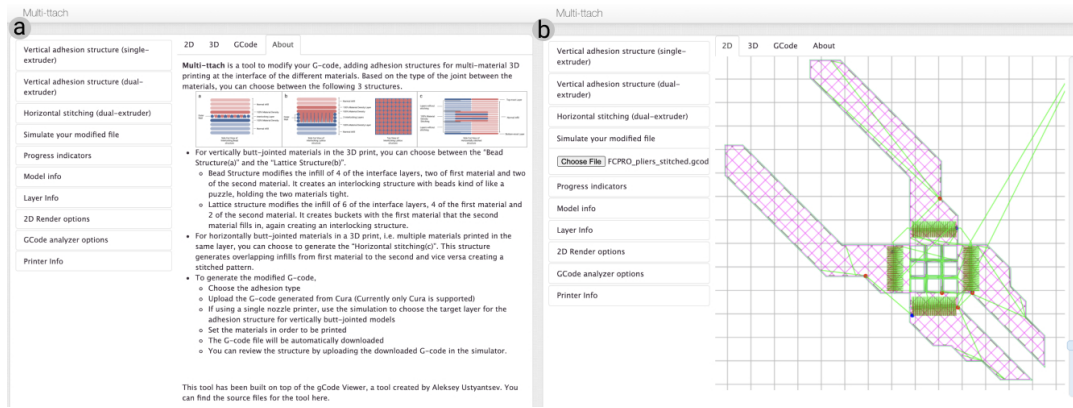


Figure 9: Using our Multi-ttach interface (a), users can upload their pre-sliced G-codes and choose the type of adhesion technique to be added to the code, and select parameters (e.g., type of machines, layer to add multi-ttach layers, etc.). After the modified G-code has been downloaded, user can simulate the modified G-code to review the added adhesion structure (b).

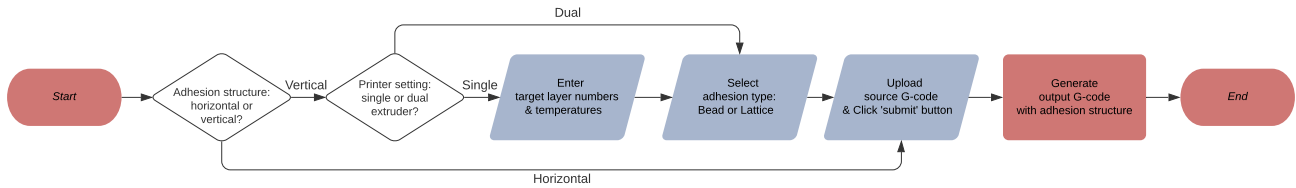


Figure 10: A flow chart of the interactive editor for users to generate a desired adhesion structure in the input G-code file

automatically visualizes the source G-code file in 2D and 3D plane to help users decide the location of the interface. In addition to the adhesion type, in (1) vertical adhesion structure with a single extruder printer, if needed, the user should enter the target layers and the corresponding temperatures by looking at the visualized 3D model layer by layer. In (3) horizontal stitching, no additional input is required. After uploading the G-code file and specifying options if needed, users click the ‘submit’ button, and the processed G-code file with adhesion structure is generated and downloaded to be saved locally. Users can also check the adhesion structure by uploading the processed G-code file in the ‘simulate your processed file’ tab to visually validate it by scrolling throughout all layers.

6 VALIDATION

In order to validate our claims, we first generated a variety of samples consisting of two mechanically distinct materials (PLA-TPU, PLA-Nylon, ABS-Conductive PLA, PETG-TPU, ABS-TPU), and empirically validated that all the samples printed with lattice and bead structures are glued tighter than the ones printed without any adhesion structure. In the case of PLA-Nylon printed in this order, the process of vertically printing samples without adhesion structures failed in being successfully printed, as the two parts fell apart without any force. The samples with the bead and lattice structure completed printing and the two materials were able to hold tight on to each other.

For further scientific evaluation, we performed uni-axial tensile testing on PLA-TPU, ABS-TPU and PETG-TPU dual material samples with three printing strategies: plain, bead, and lattice for

vertically printed samples, and two printing strategies: plain and horizontal stitch for the horizontally printed samples. PLA and TPU are two materials that are currently the most common to represent rigid and flexible filament for FDM, but have shown to have poor adhesion in many existing research and practical examples [Yusuf 2017]. With ABS and PETG being popular printing materials as well, we tested their combination with TPU. We used the ASTM D2095 standard for testing adhesion strength as a jump off point to design the testing and specimen conditions. Standard settings for this testing presented an issue as it is not designed for ‘3D printed’ polymers, e.g., the force required to pull the sample was too high and did not allow the test to last longer than 12 sec. Therefore, we modified the testing conditions as are outlined below.

6.1 Sample Preparation

Each sample was 0.5x0.5x2" in dimension with material switching at 1" of the length as shown in Figure 11a. For all samples, the layer height was 0.2mm and wall thickness was 0.8mm as is the default setting in Cura. The vertically adhered samples were printed at 50mm/s speed, while the horizontally adhered samples were printed at 60mm/s based on the printers used. All vertical adhesion samples were printed on Creality Ender 3. All horizontal adhesion samples were printed on FlashForge Creator Pro. For testing vertical adhesion, we printed samples in each condition for testing iteration, with no adhesion (P#, n=3), lattice structure (G#, n=3) and bead structure (B#, n=3). For testing horizontal adhesion, we printed samples with no adhesion (H#, n=3) and horizontal stitching (S#, n=3). For the testing purpose, we kept the infill of the samples at

100% to minimize breakage in the sections other than the interface due to weaker binding strength at lower infill. We have used AP1 - AP3, AG1 - AG3, AB1 - AB3, AH1 - AH3, AS1 - AS3 to refer to ABS and TPU samples, PP1 - PP3, PG1 - PG3, PB1 - PB3, PH1 - PH3, PS1 - PS3 to refer to PETG and TPU samples, and simply P1 - P3, G1 - G3, B1 - B3, H1 - H3, S1 - S3 to refer to PLA and TPU samples.

6.2 Apparatus

We used the Instron 4943 with pneumatic grips #2712-041 for 1 KN load cell for testing. The distance between the grips was 20mm and the pressure used was 15 psi for vertically printed samples. The lower pressure was necessary since we were using a flexible material (TPU) with higher susceptibility to compression in the machine grips. This pressure was increased to 40-60 psi in the horizontally printed samples since the samples easily slipped in the machine at lower pressures. The speed was set to 100psi/min and a small pre-load of 0.0001 KN was applied to ensure that all the samples started from 0 tensile strain after reaching the desired force. To make sure the grip of the machine held each sample at the same location (see Figure 11b), each sample was marked at 0.5" mark from the end edges (Figure 11c). We increased the speed to 200psi/min for the ABS-TPU and PETG-TPU samples after testing the PLA-TPU samples as we found that the increased speed would not affect the adhesion behavior while enabling testing in reasonable time.

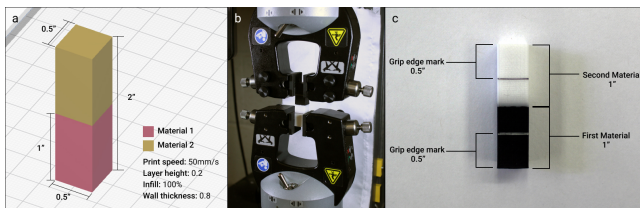


Figure 11: (a) A specification of a sample and printing parameters for vertical placement, (b) which is 3D printed and held in testing machine. (c) Dimensions of the sample and markings made to facilitate uniformity in testing.

6.3 Results

PLA-TPU: The major finding from tensile testing the vertical adhesion between PLA-TPU samples is that both the lattice and bead structures were stronger than the TPU-TPU single material bond even with 100% infill (see Figure 14a). The failures occurred in the TPU section of the bead and lattice structures samples and the interface remained intact even after breakage occurred (see Figure 12c). As for the samples with no adhesion for comparison, the three samples failed at the interface of PLA and TPU (see Figure 12b), demonstrating that the dual material adhesion, without any technique to enhance it, breaks by uni-axial force.

The graphs in Figure 13 show the maximum stress that each type of sample could endure. It can be seen from graph in Figure 13a that the samples with bead and the lattice could sustain a higher stress than the plain samples before breaking at the TPU-TPU interface. The average stress endured by samples with the bead structure was the highest at 0.86 MPa followed by samples with lattice structure at 0.64 MPa and the samples with no adhesion at 0.2 MPa. Another finding is that the horizontally stitched samples can endure a larger

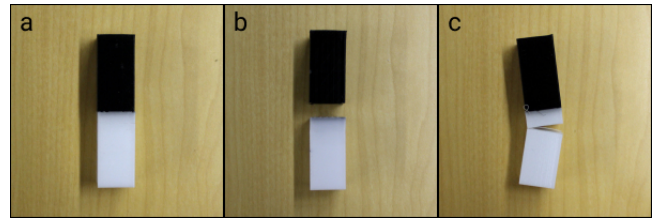


Figure 12: (a) 2" PLA (black)-TPU (white) sample. Types of failures: (b) at PLA-TPU and (c) at TPU-TPU interface

stress than the plain samples without any adhesion enhancements (see Figure 14b). Samples with horizontal stitching applied did not break but elongated in the TPU section, and 2 out of 3 ultimately slipped, while all the plain samples printed horizontally broke at the interface. Since we used a 1KN tensile testing machine, we had to stop the test for sample S1 when the machine reached its peak force. This demonstrates that horizontal stitching produces a stronger bond than having no adhesion structure since they endured a larger stress before slipping with no breakage. Graph in Figure 13b further illustrates this result, and the graphs in Figure 13 and Figure 14 summarize the result.

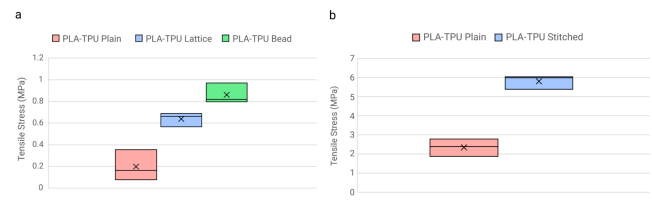


Figure 13: The maximum stress endured by vertically printed samples (a), and by horizontally printed samples (b).

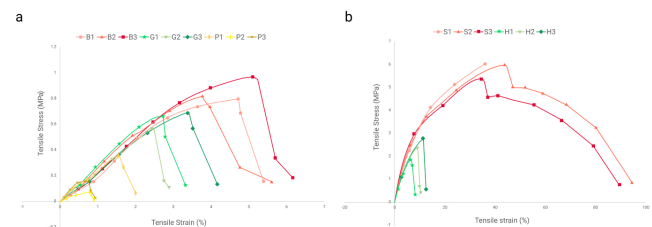


Figure 14: Stress versus strain plot of vertically printed samples in PLA-TPU (a), and horizontally printed samples (b).

ABS-TPU: We found that all the vertically printed samples either broke near the interface or in the ABS section of the sample. However, from the Figure 15a we can conclude that the bead and lattice structures endure more stress on an average than the plain samples before failure. Figure 16 shows the stress vs. strain curves of all the tested samples whereas Figure 15 shows the overview of the stress endured by the samples. The average stress endured by samples with the bead structure was the highest at 1 MPa followed by samples with lattice structure at 0.9 MPa and the samples with no adhesion at 0.36 MPa. Among the horizontal samples, all the plain samples (AH1- AH3) broke at the interface whereas the stitched samples (AS1-AS3) slipped instead of breaking as the machine reached the limit of the load cell, proving that the ABS-TPU alignment with stitching works better than having no adhesion.

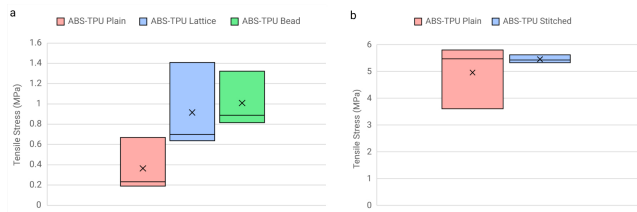


Figure 15: The maximum stress endured by (a) vertically, and (b) horizontally printed samples in ABS-TPU.

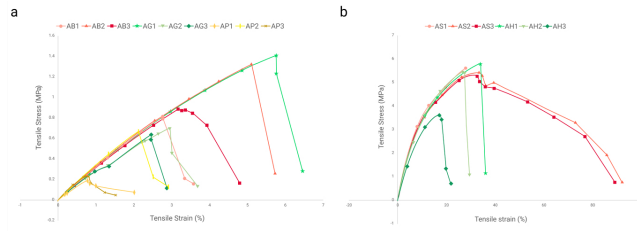


Figure 16: Stress versus strain plot of (a) vertically, and (b) horizontally printed samples in ABS-TPU.

PETG-TPU: All the vertically printed samples of the PETG-TPU combination broke at the interface except for PG3, i.e., a lattice sample which broke in the PETG section near the machine grip. Unlike PLA-TPU and ABS-TPU combinations, we can see from the graph in Figure 17a that PETG-TPU printed with the lattice structure does not differ significantly from the plain samples, while the bead structure endures more stress on an average (2.1 MPa) than both plain and lattice structures (0.5 MPa and 1MPa respectively) as illustrated in Figure 17b. For horizontally printed samples, however, we found that the samples with no adhesion behave almost similar to the stitched samples in this condition.

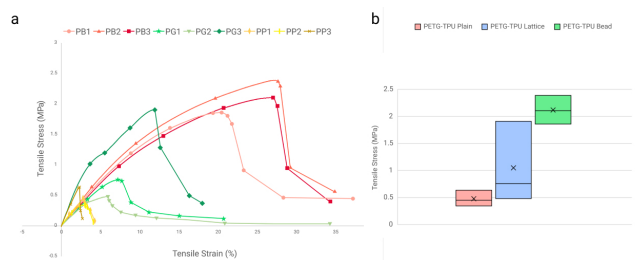


Figure 17: Stress versus strain by (a) vertically printed sample and (b) maximum stress endured before failure for vertically printed samples.

Based on all the testing performed, on an average, the bead structure endures the most stress followed by the lattice structure in the vertical samples. For horizontally printed PLA-TPU and ABS-TPU combinations, the stitched structure provides enhanced adhesion compared to having no adhesion structure. We can conclude that Multi-ttatch provided increased adhesion between the two materials in both vertical and horizontal (except PETG-TPU) orientations.

7 EVALUATION WITH APPLICATIONS

Incorporating multiple materials that impart special properties with functionality to an object, we demonstrate the application of the proposed adhesion structures.

Passive Everyday Objects with Different Material Texture:

Flip Flop. Integrating our techniques for stronger multi-material adhesion, one might desire to print an everyday use artifact such as a flip-flop designed by Thingiverse user Gyrobot [gyrobot (Thingiverse user) 2014] using multiple materials, rigid where durability is desired and flexible where the foot might touch the flip-flop for extra comfort as well as the bottom for friction while walking. Without good adhesion between the two materials, the flip-flop is likely to come apart by the regular usage resulting in wear and tear based on the poor adhesion between PLA and TPU demonstrated by a user in the demo video [jtronics (Thingiverse user) 2019]. We reprocessed the sliced file for a flip flop using the lattice structure. The flip flop is printed with TPU (white) with a few layers of PLA (black) inserted in the middle to strengthen the flip flop with its rigidity (see Figure 19).

Active Shape Changing Device: Flexy Soft Robotic Gripper.

A demo video of printing soft robotic gripper [jtronics (Thingiverse user) 2019] showed many attempts to print in various material combinations where there were lots of issues in adhesion between the flexible and rigid materials. We reprocessed the design using the interlocking bead structure to print it in TPU and PLA. The two materials stick together well even with several gripping actions triggered by the attached motor as seen in Figure 18 demonstrating the applicability of our techniques in printing objects with motion.

A Meta-material Mechanism Device: Pliers.

To demonstrate the strength of horizontal stitching in objects experiencing high stress, we printed a meta-material mechanism device [Ion et al. 2016], i.e., the pliers (Figure 20a-b). The pliers consist of different meta-materials to be operated as a machine, where the flexible part’s movement propagates to the tongs of the pliers. We employed horizontal stitching at all the PLA-TPU interfaces to ensure the adhesion of the two materials. Horizontal stitching structure only affects the inside of the model leaving the exterior aesthetics as intended, without any unexpected color gradation on the outside (see Figure 20c-e).

Other Examples in Wider Domains: Tooth Implant.

We demonstrate the potential applicability of Multi-ttatch in health-care where the potential of low-cost 3D printing has been on the rise [Diment et al. 2017]. A patients’ tooth can be 3D scanned and remodeled for custom implant modeling, where the lower part is flexible exerting lower pressure on the gums while the top is stronger and more rigid providing higher chopping and grinding power. We 3D printed a scaled up model of a tooth using TPU for the lower part and PETG for the top part of the tooth (see Figure 21). In this scenario, we played a user splitting one 3D STL model from Thingiverse [svenergy (Thingiverse user) 2016] using an existing software for slicing and then post-processing with Multi-ttatch to generate the final G-code for adhesion in PETG and TPU.

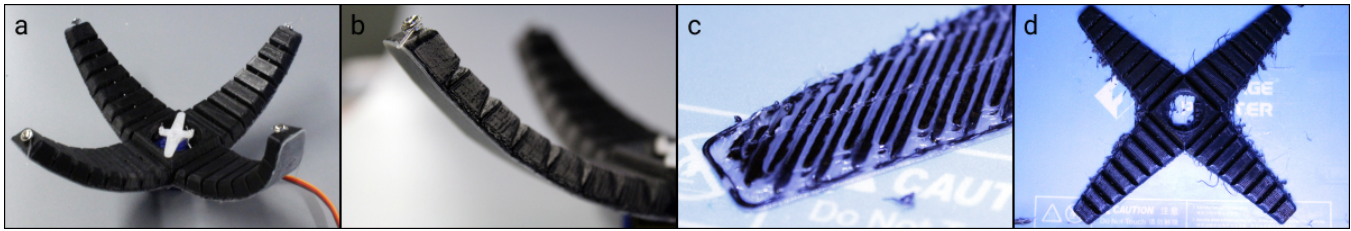


Figure 18: (a) Rigid (PLA) gripper with a flexible (TPU) base, (b) shows a close up of the two material interface, (c) shows bead interlocking structure at the interface of the two materials, (d) shows gripper printed flat.



Figure 19: (a) Flip-flop in use, (b) a close up of the material change of TPU(white)-PLA(black)-TPU(white), (c)-(e) process of creating the lattice structure: starting with the buckets, material purged into buckets, then covering with the final layer.

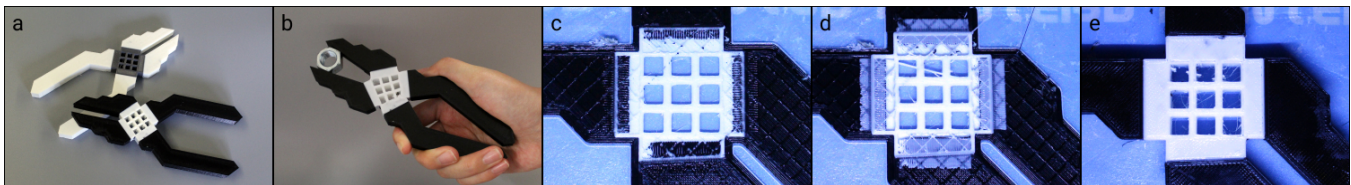


Figure 20: (a-b) Meta-material pliers printed with horizontal stitching with rigid parts in PLA and flexible parts in TPU, (c-d) two step stitching with PLA and TPU and (e) the final printed plier with the outside aesthetically untouched.

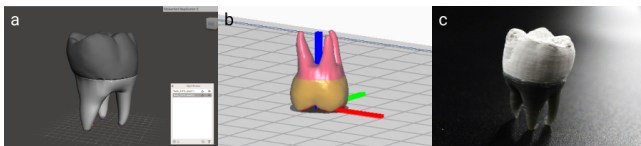


Figure 21: A process to (a) split an existing 3D file in Mesh-mixer, (b) slice into parts, and (c) 3D print in multi-material.

8 EVALUATION OF SAVED COST

We compare the saved cost (printing duration and material) in these examples below. We compare two conditions: (1) G-code simulation of the first three example application models sliced at 100% infill without any adhesion structure —which can be considered by naive users to address adhesion issues — and (2) those generated by Multi-ttach with various infill percentages that a user is likely to set in practice (15-20%) using gCodeViewer simulation [hudbrog (Thingiverse user) 2012]. As varying the density at selective layers [Tamburrino et al. 2019] is not yet available in the current slicing software and requires additional steps such as using an external software to divide the 3D model (e.g., [amagro (Instructable user) 2018]), we set the base condition with plain 100% infill for comparison as that would be the choice for naive users. As it is ideal for the human tooth model to be printed in 100%, we exclude this from the cost comparison. We do not consider the time required to change the material since it is required in all conditions and would be similar regardless of utilization of Multi-ttach. Table 1 summarizes the results.

The print time saved in the robotic gripper seems minimal since there is barely any infill density change between the two cases, with an overall geometric complexity which allows only a small space for lower infill. However, compared to their 100% infill counterparts, the flip flop and the pliers saved 34.1% and 46.8% of material, as well as decreased the print time by 67.15% and 40.2% respectively. Given that 100% infill density does not guarantee a good bond as seen from the tensile testing, the results prove that Multi-ttach has the potential to be the better alternative for many users looking to create robust but cost-effective 3D prints.

9 LIMITATIONS & DISCUSSION

Geometric Constraints to Generate Adhesion. Although Multi-ttach is available for many 3D models that may have various shapes, there exist some limitations. For vertical adhesion structures, since the bead and lattice structure require 4 and 6 layers in 0.2mm layer thickness respectively, a multi-material interface at least needs to be 0.8mm and 1.2mm. As these change the raster angles in between layers, the performance of programmable 4D printing artifacts (e.g., [Wang et al. 2019]) that utilizes printing paths for controlling curling behavior might be affected by our geometric modification. Also, the interface for the vertical adhesion structures should be parallel to the bed with the current approach. For horizontal stitching, we do not generate stitching at the top and bottom 5 layers not to hamper original appearance of the 3D model, and we observed that this strategy works better for opaque materials. However, we found that stitching might be visible through highly translucent and transparent material, affecting the overall aesthetic.

	Flip-flop		Robotic Gripper		Pliers	
	100% infill	Multi-ttach (15% infill)	100% infill	Multi-ttach (20% infill)	100% infill	Multi-ttach (20% infill)
Printing time	46hr 59min	15hr 26min	10hr 34min	10hr 28min	10hr 28min	6hr 15min
Material needed	169.45g	111.68g	56.73g	43.11g	51.32g	27.28g

Table 1: Comparison of printing time and material used for the flip-flop, gripper and pliers.

In addition to that, our current method for vertical adhesion structure assumes that adjacent layers in the target layers would not have drastic change in shape, as we generate adhesion layers based on the shape of the target layer. To utilize the proposed algorithm for organic shapes that may have complex polygons at the interfacing layers, the immediate future work will be to tackle the complexity of shapes of adjacent layers into account in generating modified adhesion structures.

Planning Printing Path in Closed Loops in One Layer. In full infill layer, we draw lines to fill an entire region of the corresponding layer perpendicular to X axis of the print bed. In this process, our algorithm follows all the points that are in the same line in y-axis and stops extruding with G0 command when the extruder moves over the empty space or outer region of the model. Since our current algorithm is not generating closed loop infill lines with minimal stroke, we found that there could be stringing issues between two regions which have empty space in between. Ideally, optimizing the printing path with the algorithm to minimize extruder travel such as fermat spirals [Zhao et al. 2016] will help minimize stringing and reduce unnecessary moves.

Choosing between Bead vs. Lattice Structure for Vertical Printing. Although both the vertical adhesion structures outperform the plain model, we found that bead structure endures more tension than lattice structure. Lattice structure can be more restricted than bead structure, as it requires at least 4 lower layers starting from the target layer, while bead structure requires only 2 layers. However, we also found that bead structure may consume more material than lattice structure in smaller objects, while it requires more printing time in larger objects because of two over-extrusion layers of bead. Thus, users can choose their desired method based on their print size and time available at their disposal.

Single vs. Dual Extruder. Multi-ttach can be used with both single and dual extruder FDM printers, however, there is a caveat. We propose using our techniques with a single extruder printer by employing the pause command in the G-code and then manually switching the filament from the nozzle. This approach works well where one only has access to a single extruder printer and needs to print objects with multiple materials attached vertically. Understandably, this approach can only be used where the number of times the material needs to be changed is low. A user cannot be expected to switch the material at every layer of the print. Horizontal stitching in particular would require changing the material at every layer where two materials are printed side by side. Such a print job on a single extruder printer however would require changing the material even if one is not employing horizontal stitching. Hence, for such print jobs, it is best to use a dual extruder printer.

Impact of Recommended Printing Temperature. Although Multi-ttach showed high efficacy in selective materials of PLA,

PETG, ABS, TPU, and Nylon, it is likely to be susceptible to adhesion issues arising due to material properties impacted by recommended printing temperature. Printing a material that requires much higher printing temperature over a material that requires lower printing temperature may need extra caution due to possibility of melting previous layer. We have also found that printing materials that are susceptible to warping such as ABS and Nylon on top of an already cooled down material may not give good adhesion results even when employing Multi-ttach. Warping of the second material introduces gaps in the print that can cause the parts to come apart easily. Our techniques work well with material combinations that print in the similar recommended temperature ranges.

Other Mechanical Testing. We performed a uni-axial tensile test on PLA-TPU, ABS-TPU and PETG-TPU samples taking some recommendations and modifying the ASTM D2095 standard that tests bonding between two materials. Other than conducting a similar test on more combinations of materials, it may be worthwhile to conduct shear testing or a form of T-peel testing for 3D printed materials depending on the application scenarios that may introduce different expected mechanical behaviors these final multi-material prints will present and the types of stresses they need to endure.

10 CONCLUSION

In this work we describe in detail three novel interlocking structures, namely, *Bead* and *Lattice* structures for vertical adhesion and *Stitching* for horizontal adhesion to enhance the adhesion between dissimilar materials in FDM context. Multi-ttach contributes to an effective improvement in multi-material adhesion available for general users with consumer-grade single or dual-extruder printers. We also provide an online interactive editor for end-users to generate the adhesion structure of their choosing on pre-sliced G-code files. Uni-axial testing of three material combinations, namely, PLA-TPU, ABS-TPU and PETG-TPU, validated the use of Multi-ttach where samples with three adhesion structures performed better than samples without adhesion structures. We also demonstrated the use of our techniques in four application contexts.

ACKNOWLEDGEMENTS

We thank Dr. Anastasia Muliana and Dr. Matt Pharr for providing expert advice and guidance with the testing equipment.

REFERENCES

- Sung-Hoon Ahn, Michael Montero, Dan Odell, Shad Roundy, and Paul K Wright. 2002. Anisotropic material properties of fused deposition modeling ABS. *Rapid prototyping journal* (2002).
- amagro (Instructable user). 2018. Change Infill Density in a Specific Section on a 3D Model for 3D Printing. <https://www.instructables.com/Change-Infill-Density-in-a-Specific-Section-on-a-3/>. (Accessed on 6/27/2021).
- Byoungkwon An, Ye Tao, Jianzhe Gu, Tingyu Cheng, Xiang 'Anthony' Chen, Xiaoxiao Zhang, Wei Zhao, Youngwook Do, Shigeo Takahashi, Hsiang-Yun Wu, Teng Zhang, and Lining Yao. 2018. Thermorph: Democratizing 4D Printing of Self-Folding Materials and Interfaces. In *Proceedings of the 2018 CHI Conference on Human Factors*

- in *Computing Systems* (Montreal QC, Canada) (CHI '18). Association for Computing Machinery, New York, NY, USA, 1–12. <https://doi.org/10.1145/3173574.3173834>
- Céline Bellehumeur, Longmei Li, Qian Sun, and Peihua Gu. 2004. Modeling of bond formation between polymer filaments in the fused deposition modeling process. *Journal of manufacturing processes* 6, 2 (2004), 170–178.
- David Braam and Ultimaker. 2017. Ultimaker Cura. <https://ultimaker.com/software/ultimaker-cura>. (Accessed on 4/3/2021).
- Builder. 2019. Dual-Feed extruder. <https://builder3dprinters.com/dual-feed/> (Accessed on 4/7/2021).
- Javaid Butt, Dominic Adaoiza Onimowo, Mohammed Gohrabian, Tinku Sharma, and Hassan Shirvani. 2018. A desktop 3D printer with dual extruders to produce customised electronic circuitry. *Frontiers of Mechanical Engineering* 13, 4 (2018), 528–534.
- Timothy J Coogan and David O Kazmer. 2017. Healing simulation for bond strength prediction of FDM. *Rapid Prototyping Journal* (2017).
- Creativity. 2018. Ender-3 3D printer. <https://www.creativity.com/goods-detail/ender-3-3d-printer>. (Accessed on 4/3/2021).
- Lucas FM Da Silva, Andreas Öchsner, and Robert D Adams. 2011. *Handbook of adhesion technology*. Springer Science & Business Media.
- Laura E Diment, Mark S Thompson, and Jeroen H M Bergmann. 2017. Clinical efficacy and effectiveness of 3D printing: a systematic review. *BMJ Open* 7, 12 (Dec. 2017), e016891. <https://doi.org/10.1136/bmjopen-2017-016891>
- Sithiprumnea Dul, Luca Fambri, and Alessandro Pegoretti. 2018. Filaments production and fused deposition modelling of ABS/carbon nanotubes composites. *Nanomaterials* 8, 1 (2018), 49.
- Michael Dwamena. 2021. Best Soluble Support Materials for 3D Printing - PVA, HIPs. <https://3dprinterly.com/best-support-materials-for-3d-printing-pva-hips-more/>. (Accessed on 3/7/2021).
- Flashforge. 2016. Creator Pro. <https://www.flashforge.com/product-detail/4>. (Accessed on 4/3/2021).
- Joseph Flynt. 2018a. Electrically Conductive Filaments: Properties, Uses, and Best Brands. <https://3dinsider.com/conductive-filament/> (Accessed on 3/13/2021).
- Joseph Flynt. 2018b. Magnetic Filaments: Properties, How to Use It, and Best Brands. <https://3dinsider.com/magnetic-filament/> (Accessed on 3/13/2021).
- A Garg, K Tai, and MM Savalani. 2014. State-of-the-art in empirical modelling of rapid prototyping processes. *Rapid Prototyping Journal* (2014).
- gyrobot (Thingiverse user). 2014. Flexy-Flip Flop. <https://www.thingiverse.com/thing:380698>. (Accessed on 4/3/2021).
- hudbrog (Thingiverse user). 2012. GCode Analyzer/Visualizer. <https://www.thingiverse.com/thing:35248>. (Accessed on 3/31/2021).
- Alexandra Ion, Johannes Frohnhofen, Ludwig Wall, Robert Kovacs, Mirela Alistar, Jack Lindsay, Pedro Lopes, Hsiang-Ting Chen, and Patrick Baudisch. 2016. Metamaterial Mechanisms. In *Proceedings of the 29th Annual Symposium on User Interface Software and Technology* (Tokyo, Japan) (UIST '16). Association for Computing Machinery, New York, NY, USA, 529–539. <https://doi.org/10.1145/2984511.2984540>
- jtronics (Thingiverse user). 2019. Robotic Flex Gripper Mixed Dual Material. <https://www.thingiverse.com/thing:3596934>. (Accessed on 3/30/2021).
- Mohammad Abu Hasan Khondoker, Asad Asad, and Dan Sameoto. 2018. Printing with mechanically interlocked extrudates using a custom bi-extruder for fused deposition modelling. *Rapid Prototyping Journal* (2018). <https://doi.org/10.1108/RPJ-03-2017-0046>
- Jeeun Kim, Anhong Guo, Tom Yeh, Scott E. Hudson, and Jennifer Mankoff. 2017. Understanding Uncertainty in Measurement and Accommodating Its Impact in 3D Modeling and Printing. In *Proceedings of the 2017 Conference on Designing Interactive Systems* (Edinburgh, United Kingdom) (DIS '17). ACM, New York, NY, USA, 1067–1078. <https://doi.org/10.1145/3064663.3064690>
- Ltd. Kyoraku Co. 2017. SMP (Shape Memory Polymer) Filament for 3D Printer. <https://www.youtube.com/watch?v=4JuHBtquPII> (Accessed on 3/13/2021).
- Kashmiri Lal Mittal and Antonio Pizzi. 1999. *Adhesion promotion techniques: technological applications*. CRC press.
- Mosaic-Manufacturing. 2017. Splitting 1 STL into 4 STLs for multi-color & multi-material 3D printing with Meshmixer. https://www.youtube.com/watch?v=xw_ClnJ1_U (Accessed on 3/14/2021).
- Mosaic-Manufacturing. 2021. Palette 3 Pro – Mosaic Manufacturing. <https://www.mosaicmfg.com/products/palette-3-pro>. (Accessed on 4/7/2021).
- nervoussystem (Thingiverse user). 2014. 2-color tree frog. <https://www.thingiverse.com/thing:329436>. (Accessed on 3/7/2021).
- Yuta Noma, Koya Narumi, Fuminori Okuya, and Yoshihiro Kawahara. 2020. Pop-up Print: Rapidly 3D Printing Mechanically Reversible Objects in the Folded State. In *Proceedings of the 33rd Annual ACM Symposium on User Interface Software and Technology* (Virtual Event, USA) (UIST '20). Association for Computing Machinery, New York, NY, USA, 58–70. <https://doi.org/10.1145/3379337.3415853>
- parakartracer (Zortrax Forum user). 2020. Dual extrusion problems. <https://forum.zortrax.com/t/dual-extrusion-problems/9569/10>. (Accessed on 7/9/2021).
- Joseph Průša. 2021. Original Prusa i3 MK3S+ - Prusa3D - 3D Printers from Josef Průša. <https://www.prusa3d.com/original-prusa-i3-mk3/>. (Accessed on 4/3/2021).
- Punished-Props-Academy. 2017. 3D Printing Rigid and Flexible Material on the Sigma Dual Extruder 3D Printer & Simplify 3D. <https://www.youtube.com/watch?v=9hix87v8LDo>. (Accessed on 3/7/2021).
- r3ND3R (Thingiverse user). 2015. Fashion Traffic Cones Collection. <https://www.thingiverse.com/thing:948045>. (Accessed on 3/7/2021).
- ramoown (Thingiverse user). 2015. Panda Dual Extrusion. <https://www.thingiverse.com/thing:640831>. (Accessed on 3/7/2021).
- Alessandro Ranellucci. 2018. Sli3er. <https://slic3r.org/>. (Accessed on 7/9/2021).
- Abinesh Kurapatti Ravi, Anagh Deshpande, and Keng H Hsu. 2016. An in-process laser localized pre-deposition heating approach to inter-layer bond strengthening in extrusion based polymer additive manufacturing. *Journal of Manufacturing Processes* 24 (2016), 179–185.
- David Roberson, Corey M Shemelya, Eric MacDonald, and Ryan Wicker. 2015. Expanding the applicability of FDM-type technologies through materials development. *Rapid Prototyping Journal* (2015).
- Gina Scala. 2020. Introducing the new Objet30 3D printer. <https://www.stratasy.com/explore/blog/2020/objet30-announcement> (Accessed on 4/7/2021).
- Simplify3D. 2019. Properties Table. <https://www.simplify3d.com/support/materials-guide/properties-table/> (Accessed on 3/13/2021).
- Mark A Skylar-Scott, Jochen Mueller, Claas W Visser, and Jennifer A Lewis. 2019. Voxlated soft matter via multimaterial multinozzle 3D printing. *Nature* 575, 7782 (2019), 330–335. <https://doi.org/10.1038/s41586-019-1736-8>
- Michelle L Smith and James FX Jones. 2018. Dual-extrusion 3D printing of anatomical models for education. *Anatomical sciences education* 11, 1 (2018), 65–72.
- Zach Smith, Marius Kintel, Adam Mayer, and Far McKon. 2011. ReplicatorG. <http://replikat.org/> (Accessed on 4/3/2021).
- Q Sun, GM Rizvi, CT Bellehumeur, and P Gu. 2008. Effect of processing conditions on the bonding quality of FDM polymer filaments. *Rapid prototyping journal* (2008).
- svenergy (Thingiverse user). 2016. human tooth model. <https://www.thingiverse.com/thing:1485531>. (Accessed on 7/8/2021).
- Yasaman Tahouni, Tiffany Cheng, Dylan Wood, Renate Sachse, Rebecca Thierer, Manfred Bischoff, and Achim Menges. 2020. Self-Shaping Curved Folding: A 4D-Printing Method for Fabrication of Self-Folding Curved Crease Structures. In *Symposium on Computational Fabrication* (Virtual Event, USA) (SCF '20). Association for Computing Machinery, New York, NY, USA, Article 5, 11 pages. <https://doi.org/10.1145/3424630.3425416>
- Haruki Takahashi, Parinya Punpongson, and Jeeun Kim. 2020. Programmable Filament: Printed Filaments for Multi-Material 3D Printing. In *Proceedings of the 33rd Annual ACM Symposium on User Interface Software and Technology* (Virtual Event, USA) (UIST '20). Association for Computing Machinery, New York, NY, USA, 1209–1221. <https://doi.org/10.1145/3379337.3415863>
- Francesco Tamburrino, Serena Graziosi, and Monica Bordegoni. 2019. The influence of slicing parameters on the multi-material adhesion mechanisms of FDM printed parts: An exploratory study. *Virtual and Physical Prototyping* 14, 4 (2019), 316–332.
- JP Thomas and JF Rodriguez. 2000. Modeling the fracture strength between fused-deposition extruded roads 16. In *2000 international solid freeform fabrication symposium*.
- tnorton (Simplify3D Forum user). 2019. Dual extruder print offset issue. <https://forum.simplify3d.com/viewtopic.php?t=12806> (Accessed on 7/9/2021).
- tSaK (Raise3D Community user). 2018. Official Raise3D Community. <https://forum.raise3d.com/viewtopic.php?t=11842> (Accessed on 7/9/2021).
- Brian N Turner, Robert Strong, and Scott A Gold. 2014. A review of melt extrusion additive manufacturing processes: I. Process design and modeling. *Rapid Prototyping Journal* (2014).
- Ultimaker. 2016. Ultimaker 3. <https://ultimaker.com/3d-printers/ultimaker-3>. (Accessed on 4/3/2021).
- Guanyun Wang, Ye Tao, Ozguc Bertug Capunaman, Humphrey Yang, and Lining Yao. 2019. A-Line: 4D Printing Morphing Linear Composite Structures. In *Proceedings of the 2019 CHI Conference on Human Factors in Computing Systems* (Glasgow, Scotland UK) (CHI '19). Association for Computing Machinery, New York, NY, USA, 1–12. <https://doi.org/10.1145/3290605.3300656>
- RPa Wool and KM O'connor. 1981. A theory crack healing in polymers. *Journal of applied physics* 52, 10 (1981), 5953–5963.
- Jun Yin, Chaohua Lu, Jianzhong Fu, Yong Huang, and Yixiong Zheng. 2018. Interfacial bonding during multi-material fused deposition modeling (FDM) process due to inter-molecular diffusion. *Materials & Design* 150 (2018), 104–112.
- Bulent Yusuf. 2017. 3D Printed Flexible Pliers Made With Dual Extrusion. <https://all3dp.com/3d-printed-flexible-pliers/>. (Accessed on 3/30/2021).
- Haisen Zhao, Fanglin Gu, Qi-Xing Huang, Jorge Garcia, Yong Chen, Changhe Tu, Bedrich Benes, Hao Zhang, Daniel Cohen-Or, and Baoquan Chen. 2016. Connected Fermat Spirals for Layered Fabrication. *ACM Trans. Graph.* 35, 4, Article 100 (July 2016), 10 pages. <https://doi.org/10.1145/2897824.2925958>